

An Analysis of Copper Enrichment on a Gold Electrocatalyst as a Method of Syngas Synthesis from CO₂

Juliet Winiecki¹ and Xuelei Guo[#]

[#]Advisor

ABSTRACT

This literary review examines the work of a distinguished research team from the University of Berkeley and the University of Toronto. The work in question was a key paper in the global search within the scientific community to find a solution to the excess of fossil fuels within the atmosphere. Specifically, this research team's focus was the electrochemical reduction of carbon dioxide to hydrogen gas and carbon monoxide. This review offers a fundamental standpoint, honing in on a specific technique that is cutting-edge in terms of technology, research, and methodology, while also being broadly applicable. The technique includes the use of a gold (Au) electrode precisely coated with a copper (Cu) monolayer, which (altogether) serves as the electrocatalyst powering the reaction. Techniques like Raman spectroscopy and cyclic voltammetry, coupled with concepts such as Molecular Orbital Theory, helped to explain the inner workings of the carbon dioxide reduction reaction. This study demonstrated that changing the amount of Cu deposited onto a Au surface affected the produced hydrogen gas (H₂) to carbon monoxide (CO) ratio. This review also considered the appropriateness of Raman spectroscopy, and whether or not it was the best technical choice given the context of this experiment. Altogether, this review uses fundamental concepts in chemistry to analyze a new method of reducing carbon dioxide, an electrochemical process that is growing increasingly relevant in today's efforts to reduce fossil fuel emissions.

Introduction

One of the most prevalent and widely discussed topics in today's politics and society is the issue of climate change. Contributing to this crisis are fossil fuels and their consequent greenhouse effect, a phenomenon by which carbon dioxide (CO₂) and other molecules cloud our skies and trap heat. Scientists have worked persistently in search of a way to try and limit the amount of greenhouse gasses in the air. One widely explored solution is carbon capture, the process of collecting CO₂ and either storing or converting it to an agent that will not affect the atmosphere.

As carbon capture started to gain more recognition, it also ignited a search for cost-efficient methods of reducing CO₂ that use renewable forms of energy and can work in great quantities. Conveniently, the field of electrochemistry can offer a wide variety of solutions, all powered by renewable and clean energy to help support a low-carbon economy¹. However, electrochemical methods of reducing CO₂ often require an electrocatalyst to speed up production. In recent years, copper electrocatalysts have drawn much attention due to their ability to synthesize hydrocarbons and alcohols directly. This ability comes from the binding energies of Cu-based materials, which are complementary to adsorbed carbon monoxide (CO*) intermediates². General methods of converting CO₂ into hydrocarbons (with a copper electrode), however, result in large overpotentials, thus impeding efficiency. In the case of all electrocatalysts, there exist some performance concerns in addition to cell efficiency that make the search for a suitable electrocatalyst so difficult⁴.

A group of scientists from the University of California, Berkeley, and the University of Toronto considered a different model of the copper electrocatalyst. Led by Peidong Yang, a professor from the Berkeley Lab, and Edward Sargent, a professor from the University of Toronto, this group of scientists proposed a unique method for the electrochemical reduction of CO₂^{4,22}. This method, as will be discussed in detail, made use of a gold electrocatalyst coated with copper atoms.

Despite the unattractiveness of synthesizing hydrocarbons using a copper electrode, there remains an option of reducing CO₂ to single-carbon products, such as carbon monoxide (CO) or formate (HCOO⁻), or generally synthesis gas (syngas). Syngas is a mixture of carbon monoxide, hydrogen gas, and occasionally other substances. These compounds appear in various ratios which can be controlled, which will be further discussed. However, the most appealing aspect of syngas is that it can be converted into other, more industrially useful compounds such as longer hydrocarbons. This makes the electrocatalytic production of syngas a widely explored method in the reduction of CO₂. This is not to say, however, that previous methods of electro-catalytically produced syngas are perfect. As Professor Peidong Yang describes, “We know of no other single electrocatalyst that combines high production rates with such wide-ranging syngas composition control.”²² Accordingly, his team of scientists researched a design for producing syngas using a gold electrocatalyst covered with a delicately administered copper monolayer while maintaining high current densities (or high production rates) at low overpotentials. They further hypothesized that varying the enrichment of copper on the gold electrocatalyst would change the electronic structure at its surface thus impacting the CO binding and ultimately providing a method for tuning the selectivity of CO electrosynthesis and the hydrogen evolution reaction (HER).

This discourse will begin by taking a closer look at the techniques used to assemble these electrodes, as well as the methods employed to analyze their properties. Additionally, this paper will focus on the extent to which Raman spectroscopy was the appropriate choice given the context of this experiment. Overall, by tunably enriching a gold electrocatalyst with copper, these scientists were able to demonstrate an energetically efficient process for producing syngas at varying ratios.

Results

Synthesizing the Cu-Enriched Au Electrocatalysts

Gold - as well as other noble metals such as silver or copper - has distinct plasmonic properties that allow it to absorb and scatter light in great magnitudes⁵. This is significant because it allows gold to form sensitive Surface-Enhanced Raman Spectroscopy (SERS) signals, making it an attractive choice for an electrode. Surface-Enhanced Raman Spectroscopy differs from Raman Spectroscopy in that the signals are magnified by 10⁵-10¹⁰ times. This technique utilizes the Raman scattering of a substance to measure its vibrational modes (or shapes in which the molecule vibrates when excited¹⁷). Raman scattering, different from Rayleigh scattering, is when the scattered light is of a different frequency than the light source. Imagine a molecule in the ground state gets hit with light from a laser (Fig. 1a). The energy from the laser is absorbed by the molecule, sending it into a “virtual” state. The molecule does not last long in this state, however, and its vibrational energy soon dissipates. Now, the vibrational energy of the molecule can either return to its original (ground) state or to a higher energy (excited) state (Fig. 1b). In the case of the molecule’s vibrational energy returning to the ground state, the light scattered is Rayleigh scattered and has the same frequency and energy as those of the laser. However, if the molecule’s vibrational energy equilibrates to an energy state higher than the ground state, the light scattered is Raman scattered and has a different vibrational frequency and lower energy than those of the laser. There is a third case where a molecule gets further excited from an already excited state, and the terminal vibrational energy is actually at the ground state. This situation also results in Raman scattered light, although it is higher in energy than that of the laser. What is most characteristic to distinguish Raman scattered light from Rayleigh scattered light is that the laser and scattered light have different energies and frequencies.

Once light is scattered from the sample it is collected by the spectrometer and passed through a series of lenses and a grating. The grating separates the scattered light based on wavelength and finally passes it through a CCD detector, transforming the light into Raman lines. These Raman lines are what make up the Raman spectra, which will be further discussed. In general, however, these Raman spectra can help distinguish certain molecules, functional groups, as well as certain molecule behaviors. In this experiment, Raman will be used to examine the binding characteristics of CO.

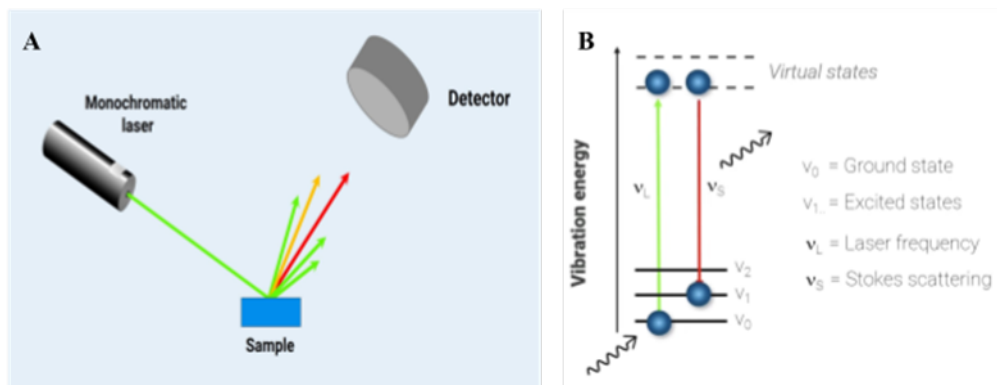


Figure 1. (a) A visual of light from a laser being shone at a sample, and the Raman scattered light being collected at a detector²³. (b) Raman scattering from a molecule in the ground state²³.

In order to optimize the signal-to-noise ratio of the Raman signals the Au electrodes needed to be cleaned and then made SERS-active, which meant they needed to undergo electrochemical roughening before Cu deposition⁶. Roughening results in increased local current density (amount of current traveling per unit of cross-section area) and reaction rate of electrodes⁷. It is generally performed through cyclic voltammetry (CV). Cyclic voltammetry is a common technique used in electrochemistry to examine the oxidation/reduction processes of a certain species^{8,9}. In a CV electrochemical cell, there are typically three electrodes: the working electrode (WE), the reference electrode (RE), and the counter electrode (CE) (Fig. 2a). The working electrode is where the reaction of interest occurs, and completes the flow of charge with the counter electrode. Therefore, whenever reduction occurs at the WE oxidation is occurring at the CE, and vice versa. The reference electrode accurately measures the applied potential by serving as a reference point. Hence, when applied potential is measured, it is usually “vs.” the reference electrode. Since the RE in our experiment is made of Ag/AgCl, the potential is measured in “V vs. Ag/AgCl”.

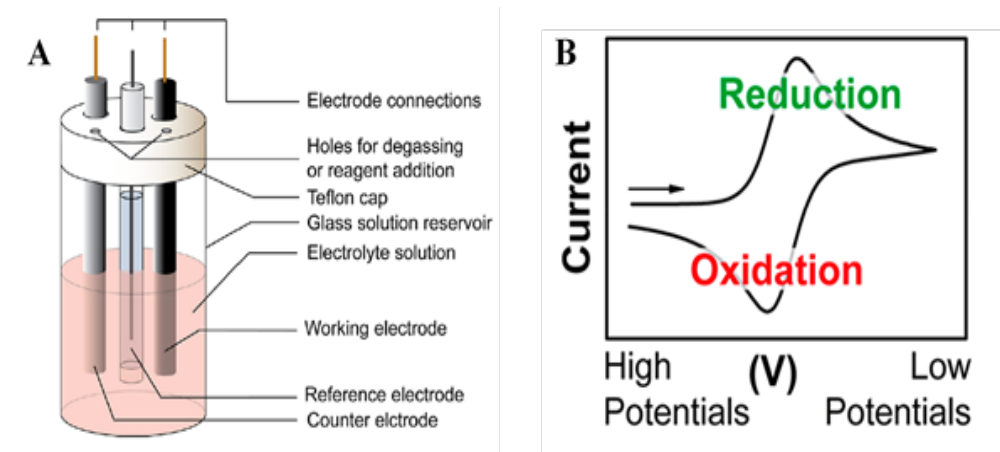


Figure 2. (a) A representation of a typical CV electrochemical cell⁹. (b) A basic voltammogram showing the direction of the cathodic sweep and the direction of the anodic sweep relative to the applied potential⁹.

The WE, CE, and RE all reside in a pool of electrolyte solution. For the roughening of the Au electrodes, the electrolyte solutions used were 0.1 M H₂SO₄ (for cleaning) and 0.1 M KCl (to make it SERS-active). Both processes - cleaning and rendering the substrate SERS-active - require numerous CV cycles. Each CV cycle includes an oxidation and reduction at the WE. This process starts at a “starting potential”, E_1 , before being swept negatively towards the “switching potential”, E_2 , at which a sufficient amount of voltage has been applied to complete the reduction process. Scan direction reverses at the switching potential, sweeping the potential in the positive direction. This cycle is completed when the starting potential is reached again. The sweep in the negative direction (from E_1 to E_2) is characterized by reduction at the WE (Fig. 2b), and therefore is called the cathodic trace. Conversely, the sweep in the positive direction (from E_2 to E_1) is characterized by oxidation at the WE (Fig. 2b) and thus is called the anodic trace. During this entire process, the current is measured with a potentiostat. Current, defined in this context by the amount of ions that travel through the solution, gives us insight into the extent of reactivity achieved with a given potential. If the current decreases, for example, we know that the amount of ions traveling from one electrode to the other is correspondingly decreasing as well. This allows us to come to the conclusion that the reduction/oxidation reaction is slowing down. This information will be useful in analyzing the cyclic voltammograms of varying Cu-enrichment.

By varying the amount of Cu on each slab, you correspondingly alter its electronic structure and properties. Therefore, in order to recognize these differences and their impact, it was essential to be able to control the amount of Cu deposition and limit it to one monolayer. The technique that this research group chose to achieve this was underpotential deposition (UPD). Unlike other forms of electrochemical deposition, UPD involves electrodeposition at a potential that is less negative (or more favorable) than the equilibrium (Nernst) potential¹⁰. This makes the deposition of one metal onto another more favorable than of that metal onto itself. This also makes the process self-terminating at a single monolayer⁴ (Fig. 3a).

Like the Au electrodes, the Cu foil used for UPD also needed to be cleaned and roughened for SERS. After following a similar process, the roughened Cu foil and Au electrodes entered the electrochemical cell along with the Ag/AgCl RE and 1mM CuSO₄, 0.5 M H₂SO₄ electrolyte solution. Thus, the CV process began, scanning across a window of 0.08 - 0.48 V vs. Ag/AgCl at a scan rate of 50 mV/s. However, in order to vary the amount of Cu deposition, they repeated this process with smaller potential windows. They included a slab with one full monolayer (purple, Fig. 3b), with a full potential window between 0.08 - 0.48 V vs Ag/AgCl. Additionally, ~2/3 monolayer (blue, Fig. 3b) and ~1/3 monolayer (orange, Fig. 3b) were included by reducing the potential window to ~0.22 - 0.48 V vs Ag/AgCl and 0.35 - 0.48 V vs Ag/AgCl, respectively. By reducing the potential window they accordingly limited the extent of reactivity thus limiting the amount of Cu deposition. In this way, the Cu-enrichment on each Au electrocatalyst was varied in a precise and accurate manner.

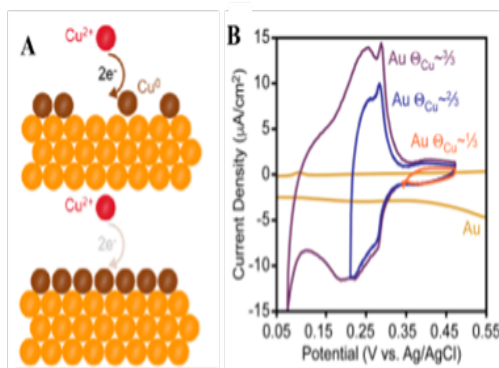


Figure 3. (a) Cu monolayer being formed on a Au surface during UPD⁴. (b) This voltammogram, taken during the UPD process, shows the different characteristics of each Cu-enriched slab with varying potential windows. The slab with a UPD window of $\sim 1/3$ only reaches a potential of about 0.35 V vs. Ag/AgCl before returning back to E_f . As a result, the current density remains relatively low throughout this process. This suggests that there was little Cu deposited onto the Au slab. For slabs with a UPD window of $\sim 2/3$ and $\sim 3/3$, however, the current densities reached great magnitudes which indicates there was a lot more Cu deposition on these slabs⁴.

Analyzing the Properties of the Electrodes & CO Binding

There are various techniques and types of cells that electrochemists use to perform CO₂RR. In this experiment, the scientists used a two-compartment H-cell (Fig. 4a) with an ion exchange membrane in the middle. H-cells are commonly used for a wide variety of processes, one of which is the reduction of CO₂. They are characterized by two separate compartments connected with a membrane¹¹. In this experiment, CO₂ was gently delivered into the cathodic compartment (on the left) while the product was collected in a gas chromatograph (not shown). Once CO₂ enters the cell, it travels toward the Cu-enriched electrode (the WE) where it undergoes the reduction half-reaction: $\text{CO}_2 + 2\text{H}^+ + 2\text{e}^- \rightarrow \text{CO} + \text{H}_2\text{O}$.

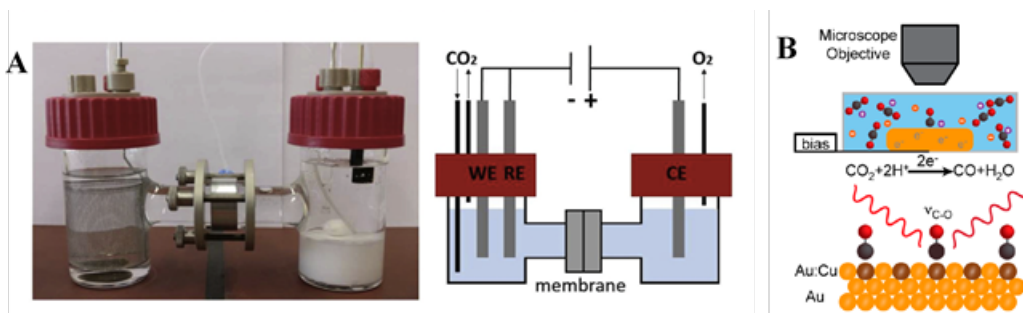


Figure 4. (a) A typical H-Cell used in CO₂RR. The products are oxygen gas and (presumably) carbon monoxide²⁴. (b) A visual of the electrochemical cell during CO₂RR with a Raman microscope mounted above⁴.

As you can see, CO is produced and adsorbed onto the electrocatalyst. While this process is happening, a Raman microscope measures the vibration of the C–O bond ($\nu_{\text{C-O}}$) in CO*. By incorporating the microscope in this cell, the chemists were able to characterize the species present by analysis of vibrational stretches, confirming the presence of CO*. As shown in Fig. 5, a fully Cu-enriched Au electrode was analyzed under a Raman microscope while varying levels of potential were applied. First, the electrode was analyzed without any bias.

In this spectrum, two peaks are observed: one around $1450/1200\text{ cm}^{-1}$ and one around 1600 cm^{-1} . These peaks are indicators of (bi)carbonate and water, respectively, which are from the electrolyte solution. But how can the Raman spectra tell us this? As mentioned, a substance's vibrational modes and chemical composition can be deduced from its Raman spectra. This is because each peak in the Raman spectra corresponds to a certain vibrational mode, which in turn is affected by the characteristics of atoms within the bond. To explain this further, one must understand that the bonds within a molecule behave like dynamic springs as opposed to static sticks. Therefore, changing the type of ball (atom) at either end of said spring (bond) will correspondingly change the way in which that molecule will move. Atomic attributes such as orientation, atomic mass, or bond order will all affect vibrational modes. Thus, although there are only a handful of vibrational modes, each molecule will produce a vibrational mode at a different frequency. For example, water in the gas phase has several peaks: one at a frequency of 1595 cm^{-1} , which comes from a bending vibrational mode; another at a frequency of 3657 cm^{-1} , which comes from a vibrational mode called the symmetric stretch; finally, the third at a frequency 3756 cm^{-1} , which comes from a vibrational mode called the antisymmetric stretch. For water, there are two hydrogen atoms and one oxygen atom that affect the vibrational modes, thus impacting the Raman spectra of gas-phase water. In this way, Raman spectroscopy can offer a deep insight into the chemical composition and vibrational modes of a certain molecule. Raman can further be utilized to distinguish a certain functional group or type of molecule, such as (bi)carbonate species and water, since past studies have shown us that these compounds have a peak at a frequency of $\sim 1450/1200\text{ cm}^{-1}$ and $\sim 1600\text{ cm}^{-1}$, respectively. From Fig. 5, we can also see that once potential is applied, there is a new peak at $\sim 2100\text{ cm}^{-1}$, credited to the presence of CO^* . As more potential is administered, the intensity and location of this peak changes, telling us that the vibration of the C–O bond ($\nu_{\text{C-O}}$) is also being affected by bias. In Fig. 5d, for example, you can see that the peaks at around 2100 cm^{-1} shift to the left with more negative potentials. This decrease in frequency is known as a red-shift, and tells us that when a negative potential is applied to the electrode (thus creating an electrostatic field around it), the frequency ($\nu_{\text{C-O}}$) in CO^* shifts. This phenomenon is also referred to as the Stark Effect. In essence, what this group of scientists demonstrated was that there were indeed (bi)carbonate and water species inside the solution and that the $\nu_{\text{C-O}}$ would shift given an applied potential.

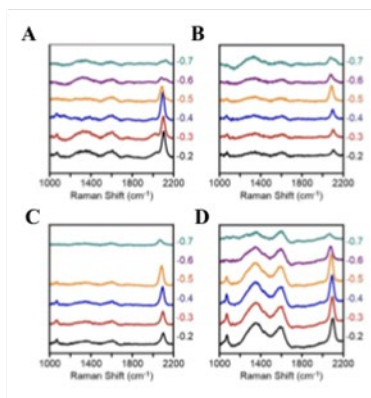


Figure 5. Shown above are the Raman spectrums of electrodes that are pure Au (a), $\sim 1/3$ Cu monolayer (b), $\sim 2/3$ Cu monolayer (c), and ~ 1 full monolayer (d)⁴.

In addition to experimenting with the effect of bias on the electrodes, the group of scientists further analyzed the effect of increasing Cu-enrichment on the red-shift of $\nu_{\text{C-O}}$. To do this they compared the $\nu_{\text{C-O}}$ at a fixed potential for varying levels of Cu-enrichment. What they found was that $\nu_{\text{C-O}}$ red-shifted when they increased Cu-enrichment, which they explained through Molecular Orbital Theory (MOT). Molecular Orbital Theory is a concept we can use to understand the behavior of a molecule. Features such as color, bond order,

bond length, stability, diamagnetism (the ability to be repelled by a magnet), and paramagnetism (the ability to be attracted to a magnet) can all be predicted through this theory. According to MOT, during the formation of a new molecule, the atomic orbitals will combine to form new orbitals called molecular orbitals. Since the electrons within these orbitals behave like waves, they will either be in-phase or out-of-phase with each other¹⁷. If you can imagine a sine or cosine graph, in-phase would mean two sine or cosine graphs have peaks and troughs appearing at the same time or place. However, if these graphs were out-of-phase then the peak of one graph would be at the trough of the other graph, and vice versa. Upon combining two in-phase graphs, constructive interference will occur and the resulting graph will have a greater amplitude. Conversely, if two out-of-phase graphs combine then destructive interference will occur, resulting in a graph with a lower or negligible amplitude. A similar occurrence happens when two atomic orbitals combine. Constructive interference will create what is called a bonding orbital while destructive interference will create an antibonding orbital¹⁷; both molecular orbitals are always created whenever two atomic orbitals combine. The atomic orbitals can also overlap in different orientations, axial or parallel, which form different types of molecular orbitals. Sigma (σ) orbitals are formed through direct or axial overlapping while pi (π) orbitals form through parallel overlapping. These types of formations will appear depending on the electron configuration of the original atoms. However, whenever a σ orbital or π orbital is present in the bonding orbital, there is also one present in the antibonding orbital (denoted by an asterisk, σ^* or π^*). Electron configurations can also be used to help build a molecular orbital diagram. Molecular orbital (MO) diagrams can tell us a considerable amount about the characteristics of a molecule, such as diamagnetism or paramagnetism which are determined by the configuration of the electrons in the MO diagram. A simplified MO diagram of an S_2 molecule is shown below. This diagram shows the electron configuration of each S atom (Fig. 6, in green) before becoming an S_2 molecule. The electron configurations within the molecular orbitals of the new molecule, S_2 , are also included (Fig. 6, in purple). In a diatomic molecule, each atom's electron configuration will typically be shown on opposite sides with the resulting molecular orbitals shown in the middle. The sulfur atom's atomic orbitals (S(AOs)), for example, are on either side of the S_2 molecular orbitals (S_2 (MOs)). For either axial or parallel combinations, there exists both bonding and antibonding orbitals, signified by a σ or π for sigma or pi bonding orbitals, or a σ^* or π^* for sigma or pi antibonding orbitals. The bonding orbital always has a lower (more favorable) energy than the antibonding orbital and is always filled first with electrons. The arrow to the left of the diagram shows the direction in which energy increases, telling us that the higher an orbital is, the higher energy it has. Finally, the top of Fig. 6 contains two terms: HOMO and LUMO. The HOMO, or the highest occupied molecular orbital, simply represents the highest orbital that contains electrons. The LUMO, or the lowest unoccupied molecular orbital, represents the lowest orbital that does not contain electrons.

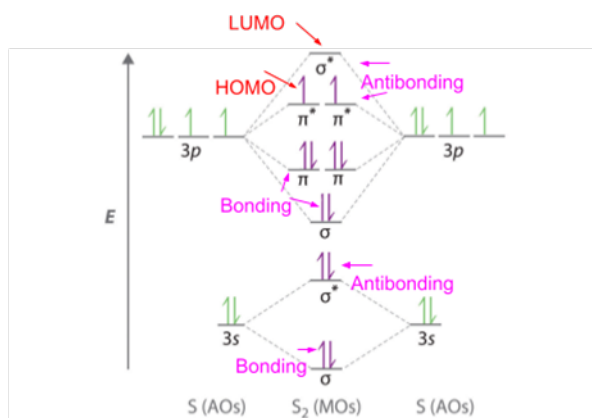


Figure 6. Shown is a molecular orbital diagram of an S_2 compound.

An understanding of Molecular Orbital Theory helps tremendously in understanding why ν_{C-O} red-shifts with increasing Cu-enrichment. The answer lies within the bond between the CO and the metal. During this interaction, CO donates electrons from its HOMO to the d-orbitals of Cu. This causes a back donation from the d-orbitals of Cu, which moves electrons into the antibonding LUMO of CO. By populating an antibonding orbital you correspondingly begin to break the bond. Accordingly, this exchange causes the C–O bond to lengthen, which alters the ν_{C-O} thus producing a red-shift in the ν_{C-O} .

In the final analysis of the Cu-enriched electrodes, the production rate of CO was compared to the production rate of H₂ with increasing Cu-enrichment. What this group of scientists hoped to find was a method of manipulating the selectivity of an electrocatalyst. Selectivity, as it relates to catalysts, is a term used to describe their ability to produce more of one product relative to other products. Chemists are making ongoing efforts in search of different ways to control the selectivity of a reaction, and research has shown that certain methods such as varying pore size or applying thin films¹⁹ suggest incredible potential in being able to enhance or control the selectivity of a catalyst. Such observations in the field of chemistry gain recognition due to the formidable potential that the capability to control the selectivity of a catalyst has. One such observation, as was demonstrated by the group of scientists, was that as the Cu monolayer coverage on a Au electrocatalyst increases, the ratio of H₂ to CO products also increases.

Analyzing the Techniques Used

Although Raman Spectroscopy is a widely used and popular analytical choice, it contains several significant disadvantages that cause some chemists to overlook this technique. In general, Raman Spectroscopy does not always work given the context of the experiment. Many compounds such as certain metals or alloys produce weak Raman signals and are not considered Raman active. This makes Raman Spectroscopy a poor choice for studying those compounds¹³. Even within the use of Raman active materials, however, there exists the possibility of fluorescence interference. Since both Raman and fluorescent light emissions stem from the same events, often a laser, there is a constant possibility that Raman signals may be interrupted by fluorescent light, which carries a stronger signal than Raman scattering and can result in an inaccurate measurement of the Raman spectra of that substance^{12,13}. Some additional disadvantages in Raman Spectroscopy are more practical, such as the involvement of costly and sensitive equipment. For these reasons, chemists have turned to a different - but complementary - analytical technique called Infrared (IR) Spectroscopy. IR Spectroscopy uses an infrared laser beam to measure the vibrational characteristics of a substance. This is measured inside a Fourier transform infrared (FTIR) Spectrometer, as shown below in Fig. 7¹⁴.

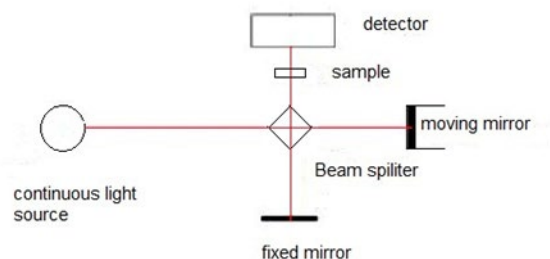


Figure 7. Shown is a visual of how the IR laser travels from the light source to the Beam Splitter, where the light is divided and travels to either the fixed mirror or the moving mirror, after which it travels back to the Beam Splitter and finally to the detector¹⁴.

As previously discussed, the bonds within molecules have distinct vibrations depending on the atoms involved, the number of bonds, and even the orientation of the bonds. We can use vibrational measurements to analyze the chemical structure of a substance. Complementary to Raman Spectroscopy, wherein a shift in vibration is measured, IR Spectroscopy measures the frequency at which a functional group (or type of molecule) has a vibrational mode (or a specific way in which the molecule vibrates). Thus, a given functional group will have a Raman shift identical to its IR peak frequency. Moreover, the electronic features of molecules that these instruments rely on are different and opposite, making these two techniques complementary to each other (in most cases). Raman scattering, for example, is influenced by the polarizability of a molecule. Raman signals tend to be more intense when associated with a molecule that has a large body of weakly bound electrons. More electronegative molecules, whose atoms hold their electrons closely, possess lower polarizability and therefore are typically not used with Raman Spectroscopy. However, they can be used with IR Spectroscopy, which works best with molecules containing a dipole moment¹⁵.

Another reason why IR Spectroscopy is generally seen as a stronger technique is because it does not have the same practical issues as Raman Spectroscopy. For one, fluorescence does not interfere with IR signals, nor do other interruptions such as particles and bubbles. However, IR Spectroscopy does contain one significant disadvantage: it is incompatible with water or moisture. Unlike Raman Spectroscopy, which possesses a limited capability of detecting water, IR Spectroscopy will detect water easily. This makes working with aqueous solutions an issue for IR Spectroscopy since water will interfere with the desired results¹³. In the context of this experiment, the ability to measure vibrational frequencies through an electrolyte solution was a crucial characteristic for determining the analytical technique of choice. Therefore, Raman Spectroscopy was the appropriate selection for examining the properties of CO*.

Discussion

From the evidence provided, it is clear that this method of controlling Cu-enrichment on an Au electrocatalyst was successful in tuning the selectivity of syngas electrosynthesis. By varying the level of Cu that was deposited onto the Au electrode, the strength of the bond between CO and metal changed. Raman spectroscopy suggested that bias might induce a red shift in the ν_{C-O} , providing insight as to how the C–O bond operates. Additionally, MOT explained this phenomenon to a further degree of specificity, helping us understand how the addition of Cu atoms affected the bond within CO. Finally, CV provided a means by which the experiment could be more precise, allowing the activation of the electrodes for Raman spectroscopy and behaving as the fundamental operator behind UPD (which again was the technique used to terminate Cu deposition at a single monolayer).

Thus, a successful method of changing the H₂:CO product ratio was found. This is notable due to the fact that selectivity is one of the most important criteria in the design of a new catalyst²⁰. Greater selectivity within a catalyst potentially reduces the cost, waste of reactants, and toxic byproducts, and even eliminates the need for expensive separation procedures²⁰. In this way, Professors Yang and Sargent demonstrated that Cu-enriched Au electrodes can fulfill their electrocatalytic responsibilities of not only providing the CO₂RR an alternative energy pathway (with lower activation energy) but also of having excellent selectivity.

This technique also maintained high current densities at low overpotentials, making it a sustainable, low-cost method and broadening its possible applicability to industrial use. As one of the scientists, Michael B. Ross explains, “If these electrocatalysts could be scaled up to work in industrial reactors, we could make syngas using renewably generated electricity and CO₂,”²². As it relates to larger CO₂ recycling systems, selectivity plays an even more significant role. Since the end goal of electrochemically produced syngas is a conversion to either smaller molecules or larger hydrocarbons - depending on the ratio of H₂:CO - a successful catalyst should have an apt ability to produce a syngas composition according to the subsequent reaction. Therefore, this Cu-enriched Au catalyst design can be implemented into a diverse range of CO₂ recycling systems.

As with all developments in science, this demonstration of a versatile catalyst can be improved upon. There is always room for higher Faradaic efficiency, higher current densities, and lower overpotentials²¹. Furthermore, it is well known that gold is an expensive and scarce material, making it a questionable choice in the large-scale reduction of CO₂. Although this method of converting CO₂ into syngas was successful, it needs to be considered that the fundamental part of this methodology relies on a material which is growing increasingly exorbitant. Thus, the future of this design may rely on metals other than gold.

Acknowledgments

I would like to thank my advisor for the valuable insight provided to me on this topic.

References

- (1) N. S. Cuellar, O. Hinrichsen, M. Fliescher, A. Rucki, K. Wiesner-Fleischer. Advantages of CO over CO₂ as a reactant for electrochemical reduction to ethylene, ethanol and *n*-propanol on gas diffusion electrodes at high current densities. *Electrochimica Acta*. 307, 164-175 (2019)
<https://doi.org/10.1016/j.electacta.2019.03.142>
- (2) H. Cui, Y. Guo, Y. Xue, Z. Zhou. Catalyst design for electrochemical reduction of CO₂ to multicarbon products. *Small Methods*. 5, 1-14 (2021)
- (3) A. Appel, M. Helm. Determining the overpotential for a molecular electrocatalyst. *ACS*. 4, 630-633 (2013)
- (4) C. Dinh, P. Luna, M. Ross, E. Sargent, P. Yang. Tunable Cu enrichment enables designer syngas electrosynthesis from CO₂. *J. Am. Chem. Soc.* 139, 9359-9363 (2017)
- (5) M. Bolshov. Characterization of labeled gold nanoparticles for surface-enhanced Raman scattering. *Molecules*. 27, 893 (2022) <https://doi.org/10.3390/molecules27030892>
- (6) W. Fu, H. Lee, J. Liao, B. Liu, J. Sitjar. SERS-Active substrate with collective amplification design for trace analysis of pesticides. *Nanomaterials*. 9, 664 (2019) <https://doi.org/10.3390/nano9050664>
- (7) A. Belle, S. Chen, D. Dahlquist, A. Ivanovskaya, R. Lozada, F. Qian, V. Tolosa, A. Tooker, A. Yorita. Electrochemical roughening of thin-film platinum for neural probe arrays and biosensing applications. *J. Electrochem. Soc.* 165 (2018)
- (8) J. Dempsey, T. Eisenhart, N. Elgrishi, B. Mccarthy, E. Rountree, K. Rountree. A practical beginner's guide to cyclic voltammetry. *J. Chem Educ.* 95, 197-206 (2017)
- (9) Gamry Instruments. CV-cyclic voltammetry.
<https://www.gamry.com/electrochemistry-applications/cv-cyclic-voltammetry>
- (10) Academic accelerator, Underpotential deposition.
<https://academic-accelerator.com/encyclopedia/underpotential-deposition>

- (11) A. Bard, G. Inzelt, F. Scholz. Electrochemical dictionary. Springer, Berlin, Heidelberg. (2008)
https://doi.org/10.1007/978-3-540-74598-3_8
- (12) Mettler Toledo. https://www.mt.com/us/en/home/applications/L1_AutoChem_Applications/Raman-Spectroscopy/raman-vs-ir-spectroscopy.html#applications
- (13) H. Vaškova. A powerful tool for material identification: Raman spectroscopy. *International Journal of Mathematical Models and Methods in Applied Sciences*. 5, 1205-1212 (2011)
- (14) P. M. V. Raja, A. Barron. IR spectroscopy. *Chemistry LibreTexts*. 4.2.
[https://chem.libretexts.org/Bookshelves/Analytical_Chemistry/Physical_Methods_in_Chemistry_and_Nano_Science_\(Barron\)/04%3A_Chemical_Speciation/4.02%3A_IR_Spectroscopy](https://chem.libretexts.org/Bookshelves/Analytical_Chemistry/Physical_Methods_in_Chemistry_and_Nano_Science_(Barron)/04%3A_Chemical_Speciation/4.02%3A_IR_Spectroscopy)
- (15) P. M. V. Raja, A. Barron. IR spectroscopy. *Chemistry LibreTexts*. 4.3
[https://chem.libretexts.org/Bookshelves/Analytical_Chemistry/Physical_Methods_in_Chemistry_and_Nano_Science_\(Barron\)/04%3A_Chemical_Speciation/4.03%3A_Raman_Spectroscopy](https://chem.libretexts.org/Bookshelves/Analytical_Chemistry/Physical_Methods_in_Chemistry_and_Nano_Science_(Barron)/04%3A_Chemical_Speciation/4.03%3A_Raman_Spectroscopy)
- (16) G. McLaskey, S. Cebry, J. Song, V. Eynon, B. Wu, C. Ke. Structural vibrations. *McLaskey Research Group*. <https://courses.cit.cornell.edu/mclaskey/vib/struct/Koppi/modesOfVibrations.html>.
- (17) P. Flowers, K. Theopold, R. Langley. Molecular orbital (MO) theory (review). 2.2.
[https://chem.libretexts.org/Courses/Sacramento_City_College/SCC%3A_Chem_420_-_Organic_Chemistry_I/Text/02%3A_Structure_and_Properties_of_Organic_Molecules/2.02%3A_Molecular_Orbital_\(MO\)_Theory_\(Review\)#:~:text=Molecular%20orbitals%20are%20combinations%20of,2](https://chem.libretexts.org/Courses/Sacramento_City_College/SCC%3A_Chem_420_-_Organic_Chemistry_I/Text/02%3A_Structure_and_Properties_of_Organic_Molecules/2.02%3A_Molecular_Orbital_(MO)_Theory_(Review)#:~:text=Molecular%20orbitals%20are%20combinations%20of,2)
- (18) Physics Open Lab. Water molecule vibrations with Raman spectroscopy. (2022)
<https://physicsopenlab.org/2022/01/08/water-molecule-vibrations-with-raman-spectroscopy/>
- (19) S. Suib. Selectivity in Catalysis. *American Chemical Society*. (1993)
- (20) Zaera Research Group. Selectivity in Catalysts. *UC Riverside*. <https://zaeralab.ucr.edu/selectivity-catalysis>
- (21) Jhong H., Ma S. Kenis P. Electrochemical conversion of CO₂ to useful chemicals: current status, remaining challenges, and future opportunities. *Current Opinion in Chemical Engineering*. 2, 191-199. (2013)
- (22) Yang S. Scientists fine-tune system to create 'syngas' from CO₂. *Berkeley Lab*. (2017)
- (23) Bruker. Guide to Raman spectroscopy. *Raman Basics*. (2023)
<https://www.bruker.com/en/products-and-solutions/infrared-and-raman/raman-spectrometers/what-is-raman-spectroscopy.html>
- (24) Gawel A., Jaster T., Siegmund D., Holzmann J., Lohmann H., Klemm E., Apfel U. Electrochemical CO₂ reduction - the macroscopic world of electrode design, reactor concepts & economic aspects. *iScience*. 25, 1-36. (2022)